*Frontiers of Environmental Science & Engineering*
2025, 19(12): 163 https://doi.org/10.1007/s11783-025-2083-7

RESEARCH ARTICLE

# Photocatalytic membrane treatment of antibiotics: combined chemical and toxicological evaluation of effectiveness

**Martin Schmidt ✉ [1], Silke Aulhorn[2], Amira Abdul Latif[1], Martin Krauss[3], Mechthild Schmitt-Jansen[2], Daniel Breite[1], Eberhard Küster[2], Agnes Schulze[1]**

1. Leibniz Institute of Surface Engineering (IOM), Permoserstr. 15, 04318 Leipzig, Germany
2. Department Ecotoxicology, Helmholtz Centre for Environmental Research – UFZ, Permoserstr. 15, 04318 Leipzig, Germany
3. Department Exposure Science, Helmholtz Centre for Environmental Research – UFZ, Permoserstr. 15, 04318 Leipzig, Germany

## HIGHLIGHTS

- Photocatalytic polymer membrane effectively removed three antibiotics from water.
- Degradation process was monitored by combined chemical and toxicological approach.
- Initial detoxification is followed by resurgence of algal photosynthetic inhibition.
- Membrane photoaging products limiting the overall detoxification effectiveness.

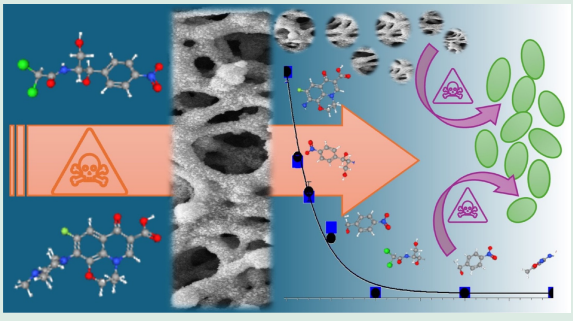

**ABSTRACT:** Antibiotic residues in wastewater promote the emergence of resistant bacteria, posing a serious potential threat to human health and ecosystems. Effective degradation strategies are crucial for removing antibiotics from wastewater. In this study, a photocatalytic polymer membrane was used to treat three antibiotics, *i.e.*, sulfamethoxazole, chloramphenicol, and ofloxacin. In parallel with chemical analysis, the acute and chronic toxicity of the antibiotics and their degradation mixtures to the freshwater green alga *Scenedesmus vacuolatus* was assessed. Photocatalytic membrane treatment of 10 mg/L aqueous solutions (and 1100 mg/L for ofloxacin) achieved complete parent-compound removal, with half-lives ranging from 6.2–102.3 min. Toxicity measured at successive irradiation times revealed initial detoxification followed by increased toxicity due to transformation products and by-products caused by membrane photoaging, limiting the total detoxification effectiveness. The results underscore the promise of photocatalytic membranes for antibiotic removal while highlighting the critical importance of photostable polymer–photocatalyst materials to prevent secondary ecotoxicological effects in water treatment applications. These results further demonstrate the need to combine chemical and toxicological methods to validate new technologies for wastewater treatment.

**KEYWORDS:** Micropollutant degradation, Polymer membrane, Photocatalysis, Ecotoxicology, Microalgae, WWTP

✉ Corresponding author. E-mail: martin.schmidt@iom-leipzig.de

Article history: Received 27 May 2025, Revised 15 July 2025, Accepted 14 August 2025, Available online 5 September 2025

# 1 Introduction

Antibiotics (AB) are indispensable agents for treating bacterial infections, making them one of the most extensively utilized pharmaceutical classes worldwide (Hutchings et al., 2019). In addition to therapeutic applications, AB play a crucial role in livestock farming (Gustafson and Bowen, 1997), including aquaculture prophylaxis (Chen et al., 2020). Abdallah et al. (2024) reported that almost 70% of veterinary medicines used in Germany are AB, which is roughly the same proportion that is used in human healthcare. The misuse and overuse of antibiotics have precipitated a global health crisis in the form of antimicrobial resistance (WHO Scientific Working Group, 1983; Murray et al., 2022). As contaminants of emerging concern, they also adversely affect nontarget organisms in aquatic ecosystems such as algae (Kümmerer, 2009). Freshwater green algae are not the primary target organisms of antibiotics; however, their position in aquatic ecosystems as primary producers and the steady inflow of AB into creeks and rivers via wastewater treatment plants (WWTPs) and nonpoint contamination sources might have long-term effects on ecosystems. Other major sources of antibiotic contamination include agricultural runoff from livestock farms and effluents from hospitals and industrial wastewater treatment plants (Rodriguez-Mozaz et al., 2015). Once introduced, antibiotics can persist in aquatic environments and are often detected in the ng/L to µg/L range (Maghsodian et al., 2022). Such a low-dose steady inflow is usually seen as pseudo-persistent contamination. Thus, AB may have ample time to affect all kinds of organisms since their modes of action are multiple, but many affect general endpoints such as protein synthesis (Halling-Sorensen, 2000).

Kovalakova et al. (2020) reviewed eight key AB of great concern, based on their consumption, detection in surface water, and ecotoxicity, including ofloxacin (OFX, a fluoroquinolone racemic mixture comprising levofloxacin and dextrofloxacin) and sulfamethoxazole (SMX, a sulfonamide). Furthermore, chloramphenicol (CAP) is a potent broad-spectrum AB with restricted use due to severe side effects such as aplastic anemia (Balbi, 2004). The German Environment Agency compiled a database titled "Pharmaceuticals in the environment" (UBA, 2021), which collects globally measured environmental concentrations (Fig. 1). For 95% of the data, the concentrations were below 10 µg/L (OFX: 9.8 µg/L; SMX: 4.0 µg/L; CAP: 2.1 µg/L). However, in heavily contaminated wastewater, peak concentrations of high µg/L to mg/L were measured. Particularly high levels have been detected in pharmaceutical production facilities, animal farms, hospital wastewater and occasionally urban wastewater. For example, SMX has been detected at concentrations of up to 9.1 mg/L in pharmaceutical industry wastewater (Dolar et al., 2012) and up to 14.1 mg/L in Mexican pig farm wastewater samples (León-Aguirre et al., 2019). OFX was found up to 318 µg/L in Nigerian hospital wastewater effluent (Ajibola et al., 2021), and CAP was detected up to 442 µg/L in liquid manure from swine feedlots in China (Li et al., 2018). Production sites and places with high consumption of antibiotics are at particular risk of environmental pollution, often

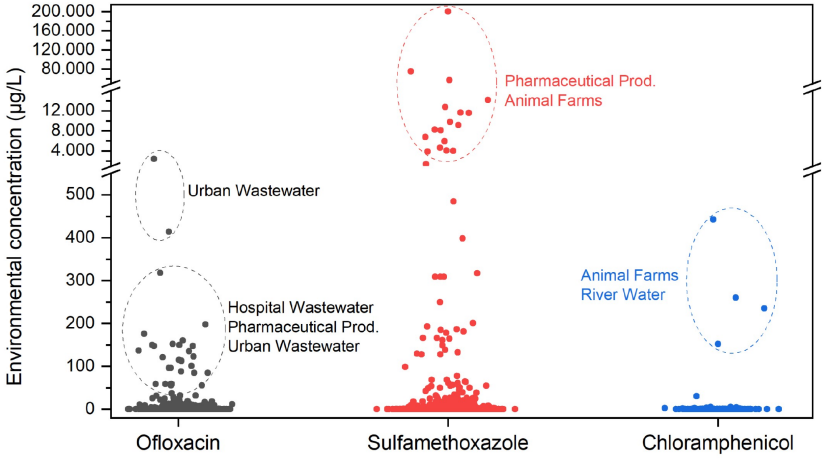


**Fig. 1** Measured environmental concentrations of ofloxacin (1169 entries), sulfamethoxazole (3521 entries), and chloramphenicol (226 entries) in aqueous samples. Data were compiled from UBA (2021) with the following database filter criteria: type of analyte: parent; detection: only positive; standardized unit: µg/L, *i.e.,* aqueous; literature credibility: good. Please note the brakes in the *y*-axis.

characterized by the presence of other contaminants, which can lead to even more harmful mixture effects (Coulibaly et al., 2025).

Effective remediation of antibiotic contaminants is essential for safeguarding the health of humans and ecosystems. The half-life of SMX and OFX in natural surface waters was estimated to be 20.3 and 10.6 d, respectively, with only limited removal in conventional WWTPs (Felis et al., 2020). Advanced wastewater treatment technologies include chemical and biological methods, adsorption, advanced oxidation processes (AOPs) such as ozonation or photocatalysis, and membrane technology (Homem and Santos, 2011). AOPs have emerged as especially promising, demonstrating the ability to degrade AB and reduce the levels of AB resistance genes (Li et al., 2023a). Integrated treatment strategies, *i.e.*, combining AOPs with biological, membrane, or adsorption processes, offer a capable approach to substantially reduce effluent toxicity further and enhance contaminant removal (Nasrollahi et al., 2022). Titanium dioxide ($TiO_2$) is an established photocatalyst explored for the removal of various forms of emerging contaminants, such as nanoparticles (Krakowiak et al., 2021) or laser-crystallized nanotubes (Bernhardt et al., 2024). The integration of $TiO_2$ with polymer membranes as a photocatalytic membrane reactor eliminates the need for subsequent catalyst separation, allowing the effective degradation of persistent pollutants such as steroid hormones at environmental concentrations (Lotfi et al., 2022). In principle, the removal mecha-nism involves the generation of electron–hole pairs due to UV irradiation and the formation of reactive oxygen species (ROS), followed by the oxidative degradation of organic contaminants (Krakowiak et al., 2021). To date, only a limited number of studies have explored the efficacy of photocatalytic polymer membranes for the degradation of AB by assessing mostly their chemical removal profile (Chin et al., 2023). However, for a reliable risk assessment of degradation processes, combining chemical and toxicological evaluations is highly important (Schmitt-Jansen et al., 2007; Rodil et al., 2009).

In this study, a combined chemical and bioanalytical approach was used to demonstrate the effectiveness of photocatalytic polymer membranes containing $TiO_2$ nanoparticles. The concentrations of three antibiotics from distinct classes, namely, sulfamethoxazole, ofloxacin, and chloramphenicol, were chosen on the basis of previously determined adverse effects on the freshwater alga *Scenedesmus vacuolatus* to follow the degradation process from a toxicological perspective. Treated solutions were tested for phytotoxicity and the degradation process was monitored in parallel via high-performance liquid chromatography. Finally, transformation products were identified via high-resolution mass spectrometry to correlate degradation stages with changes in algal toxicity.

## 2 Materials and methods

### 2.1 Photocatalytic degradation of antibiotics

Photocatalytic membranes were prepared as described elsewhere (Fischer et al., 2018). Briefly, polyvinylidene fluoride membranes (PVDF, 0.22 µm, Durapore, Merck Millipore, USA) were dip-coated with a $TiO_2$ nanoparticle suspension freshly produced in a hydro-thermal process. Membrane samples were washed 4 × 30 min in Milli-Q water and dried in air. A comprehensive characterization can be found in previous work (Fischer et al., 2018). For degradation tests, chloramphenicol (CAP, CAS 56-75-7, > 98%, Sigma-Aldrich), ofloxacin (OFX, CAS 82419-36-1, 99%, Sigma-Aldrich), sulfamethoxazole (SMX, CAS 723-46-6, > 98%, Supelco), and photocatalytic membranes (Ø = 33 mm) in petri dishes were used. A volume of 4 mL of AB in ultrapure water (Milli-Q) was added, and dark adsorption was performed overnight. The samples were subsequently irradiated via an LED lamp (365 nm, UVECO, Germany) with an irradiance of (260 ± 22) W/m$^2$ and shaken at 200 r/min (MHR 23, DITABIS, Germany). At regular time intervals (0, 15, 30, 60, 120, 240, and 360 min), aliquots of 100 µL were taken and stored at 4 °C until further measurement. Before each sampling, evaporation was determined by weighing and compensated for by adding water. Irradiation of AB solutions without a membrane or photocatalyst was performed as a control ("photolysis"). All the measurements were performed in duplicate (Supplementary material, Table S1). In addition, total organic carbon (TOC) was measured in triplicate before dark adsorption and after 360 min to assess the formation or removal of any organic byproducts from the AB or the photocatalytic membrane itself (DIMATOC 2000, DIMATEC Analysentechnik, Germany).

### 2.2 Chemical analysis of antibiotics

The parent AB concentration was determined via high-performance liquid chromatography (HPLC, Dionex UltiMate 3000, Thermo Fisher Scientific, USA) with a UV–VIS detector. The detection wavelengths were set at 210 nm (SMX), 275 nm (CAP), or 225 nm (OFX).

The mobile phase was a mixture of acetonitrile and water (30:70 v/v) with 0.5% trifluoroacetic acid. The separation was run in isocratic mode on a biphenyl column (Kinetex 5 µm 100 Å, 250 × 4.6 mm, Phenomenex) at 30 °C. The retention times were 5.01 min (SMX), 5.95 min (CAP), and 3.71 min (OFX). Chromatograms were monitored and analyzed with Chromeleon software ver. 6.80 SR14. The relative concentration $[A] = C_t/C_0$, with $C_t$ or $C_0$ being the concentration at time $t$ or after dark adsorption, respectively, was used for plotting and determining kinetic parameters. For this, the general rate law of a unimolecular reaction of order $n$ (Eq. (1)) can be integrated (Eq. (2)) and rearranged to give the integrated rate law for reactions of $n^{\text{th}}$ order (Eq. (3)):

$$-\frac{\mathrm{d}[A]}{\mathrm{d}t} = k[A]^n, \tag{1}$$

$$\int_{[A]_0}^{[A]} \frac{\mathrm{d}[A]}{[A]^n} = -k\int_0^t \mathrm{d}t, \tag{2}$$

$$[A] = \left([A]_0^{\,1-n} + (n-1)kt\right)^{\frac{1}{1-n}} (n \neq 1), \tag{3}$$

where $k$ is the apparent rate constant of the reaction with dimension $[\mathrm{mol}^{1-n}\mathrm{L}^{n-1}\mathrm{s}^{-1}]$. This approach provides the benefit of fitting a fractional-order kinetic model, which was found to be common in photocatalytic degradation (Wang, 2018). For evaluation, nonlinear fitting was performed via OriginPro (ver. 2024b, OriginLab, USA). In the case of $n = 1$ (first/pseudo-first-order reaction), integration results in the well-known Eq. (4) (with $[A]_0 = C_{t,0}/C_0 = 1$) and its linearized form in Eq. (5):

$$[A] = [A]_0\ \mathrm{e}^{-kt}, \tag{4}$$

$$\ln[A] = \ln\frac{C_t}{C_0} = -kt. \tag{5}$$

### 2.3 Algal toxicity assay

A high-throughput algal toxicity assay was performed based on the OECD (2006) guideline No. 201 (Freshwater Alga Growth Inhibition Test) and adapted by Rummel et al. (2022). Detailed information about algae cultivation and assay operation is described elsewhere (Schmitt-Jansen et al., 2007; Rummel et al., 2022). Briefly, a dilution series of AB in water (1:1.8, 10 dilution steps) was mixed with 15 µL of algae suspension (*Scenedesmus vacuolatus),* leading to a total volume of 150 µL per well (96-well plate, final algae density of ~7.5 × $10^4$ cells/mL). The plates were illuminated for 24 h at 300 r/min and 28 °C (Multitron incubator, INFORS, Germany). The negative control consisted of GB culture medium, while the herbicide Diuron (CAS 330-54-1, > 98%, Sigma-Aldrich) was used as a positive control. After 2 and 24 h of exposure, the following endpoints were measured: (1) chlorophyll *a* autofluorescence as a proxy for biomass and thus growth inhibition (fluorescence reader Spectra Max Gemini EM, Molecular Devices, USA); and (2) photosynthetic capacity (maximum and effective quantum yields, Yield I and Yield II, respectively) employing a chlorophyll fluorometer (Imaging PAM, M-series, Heinz Walz, Germany). Relative inhibition compared to controls was calculated and plotted against the HPLC-measured concentration of AB. Finally, the $E_{\max}$ model (Eq. 6), as a generalization of the Hill equation, was used to determine effect concentrations (EC) by fitting the sigmoidal dose–response relationships (Macdougall, 2006):

$$E = E_0 + \frac{E_{\max} \times C^S}{EC_{50}^S + C^S}, \tag{6}$$

where $E$ is the observed effect, $E_0$ is the baseline effect, $E_{\max}$ is the maximum effect, $C$ is the concentration of the toxicant, $EC_{50}$ is the concentration producing a 50% maximal effect (inflection point of the curve), and $S$ is the slope (Hill coefficient). For evaluation, nonlinear fitting was performed via OriginPro ver. 2024b.

To assess the change in toxicity at successive degradation stages, samples were collected at different irradiation times to profile the removal curve of the parent AB compound. Ultrapure water (Milli-Q) was used as a control to evaluate potential effects attributable solely to the photocatalytic PVDF membrane. When necessary, the sample pH was adjusted to about 6.0–7.0 using 5 or 2.5 mol/L NaOH. All measurements were performed in quadruplicate and are given as mean and standard deviation (Supplementary Material, Tables S2 and S3).

### 2.4 Identification of transformation products (TPs)

Samples after specific duration of UV irradiation were analyzed by liquid chromatography coupled with high-resolution mass spectrometry (LC-HRMS; Thermo Ultimate 3000, quadrupole-Orbitrap Thermo QExactive Plus, electrospray ionization in positive and negative ion mode). Irradiation times were chosen to profile the removal curve ($C/C_0$ of approximately 100%, 75%, 50%, 25%, and 0% within the algal assay and after the total time of 360 min). LC separation was conducted via a gradient elution program as described elsewhere (Rigano et al., 2025). For analysis, a full scan acquisition (m/z 80–1200, nominal resolving power:

70,000) was combined with four data-dependent MS/MS scans (top 4 full scan intensities, nominal resolving power: 35,000). An inclusion list of the parent AB and suspected TPs compiled from the literature was used – SMX: Hernández-Tenorio (2024); CAP: Giri and Golder (2018), and Xu et al. (2019); OFX: Peres et al. (2015), and Rodríguez et al. (2015). The expected ion m/z values for the positive ($M+H^+$) and negative modes ($M–H^–$) were calculated from the molecular structures, and the retention times were predicted using RTpred 1.0 via a model trained on 850 environmental compounds of diverse chemical classes and structures.

For TP identification, first, Thermo raw files were converted to mzML files (ProteoWizard, Chambers et al., 2012). Subsequently, peak detection and annotation were conducted in MZmine 4.2.0 (Schmid et al., 2023). The processing steps are provided in the Supporting Information (Table S4). For confirmation of TPs annotated tentatively based on m/z (7 ppm window) and retention time (predicted RT ± 2.5 min), MS/MS spectra were exported in mgf format and processed via SIRIUS 5.8.6 software (Dührkop et al., 2019), which allows experimental spectra to be matched with those predicted from the TP structure using the tool CSI-FingerID (Dührkop et al., 2015). The SIRIUS settings are given in the Table S5.

## 3 Results and discussion

### 3.1 Algal toxicity of antibiotics

An algal toxicity test with AB was performed to determine a suitable starting concentration for photocatalytic degradation experiments. Figure 2 shows the effects of AB concentration on SMX, CAP, and OFX. The data were fitted via the $E_{max}$ model (Eq. 6) with the resulting model parameters listed in the Supporting Information (Table S6). In general, the EC values of the individual AB determined within this study were higher than the typical concentrations found in the environment, but they partly remained within the levels observed in heavily contaminated wastewater (especially for SMX, see Fig. 1).

The data revealed distinct differences among the three AB. While SMX and CAP had similar chronic toxic effects on population growth inhibition in the range of 40 µmol/L (10–13 mg/L, respectively), OFX was about 50-times less toxic, with an $EC_{50}$ of approximately 2000 µmol/L (~725 mg/L). Other algal toxicity studies with exposure times between 24 and 72 h determined $EC_{50}$ values of 1.6 mg/L for SMX using *Chlorella vulgaris* (Baran et al., 2006), 4.1 mg/L for CAP (Kusk et al., 2018), and > 120 mg/L for levofloxacin (González-Pleiter et al., 2013), both of which use *Pseudokirchneriella subcapitata* (renamed *Raphidocelis subcapitata*). However, a review on the toxicity of fluoroquinolones to freshwater organisms revealed substantial species-specific disparities, with $EC_{50}$ values ranging from low to mid mg/L (Pauletto and De Liguoro, 2024).

In this study, SMX led to a maximum growth inhibition of 60%. SMX disrupts folic acid biosynthesis by competitively inhibiting dihydropteroate synthase, an enzyme responsible for converting *p*-aminobenzoic acid to dihydrofolic acid (Smilack, 1999). Guo et al. (2021) also reported a growth inhibition rate of ~63% after 7 d of incubation with 300 µg/L using *Raphidocelis subcapitata*. It was concluded that effects on green algae are not caused primarily by folate biosynthesis inhibition but rather are more likely due to genotoxicity and DNA damage, since transcriptome analysis revealed differentially expressed genes for DNA replication and repair processes, as well as for chlorophyll, photosynthesis, and ribosome biogenesis.

The maximum quantum yield after 2 and 24 h also differed among the three AB. All AB affected the photosystem after 24 h of exposure, with CAP (~14 µmol/L) being the most effective, followed by SMX (~25 µmol/L) and OFX (~340 µmol/L; again, the least toxic AB from the three tested). While all three AB did show chronic toxicity effects (24 h of exposure) on both photosystem endpoints, only CAP and OFX were already effective after short-term exposure for 2 h (Fig. 2). Studies on *Selenastrum capricornutum* have indicated that SMX can inhibit photosynthetic electron transport but also induces uncoupling of the thylakoid membrane, which is the main place of photosynthesis (Liu et al., 2011). CAP inhibits protein biosynthesis by binding to the 23S rRNA of the 50S ribosomal subunit, indirectly disrupting algal photosynthesis by impairing chloroplast ribosomes, leading to alterations in biochemical components, *e.g.*, lipid peroxidation and a decrease in protein content (Xiong et al., 2019). Thus, effects on photosynthesis are likely to occur faster. For both SMX and CAP, a stimulation of photosynthetic capacity after 24 h at concentrations below the $EC_{10}$ was observed. These stimulatory responses are often mediated by mild oxidative stress, which enhances pigment synthesis and photosynthesis-related gene expression (Liu et al., 2017). OFX inhibits nucleic acid biosynthesis by acting on DNA gyrase and topoisomerase IV, enzymes crucial for DNA replication and transcription (Monk and Campoli-Richards, 1987). Studies on tomato (*Solanum lycopersicum*) indicated

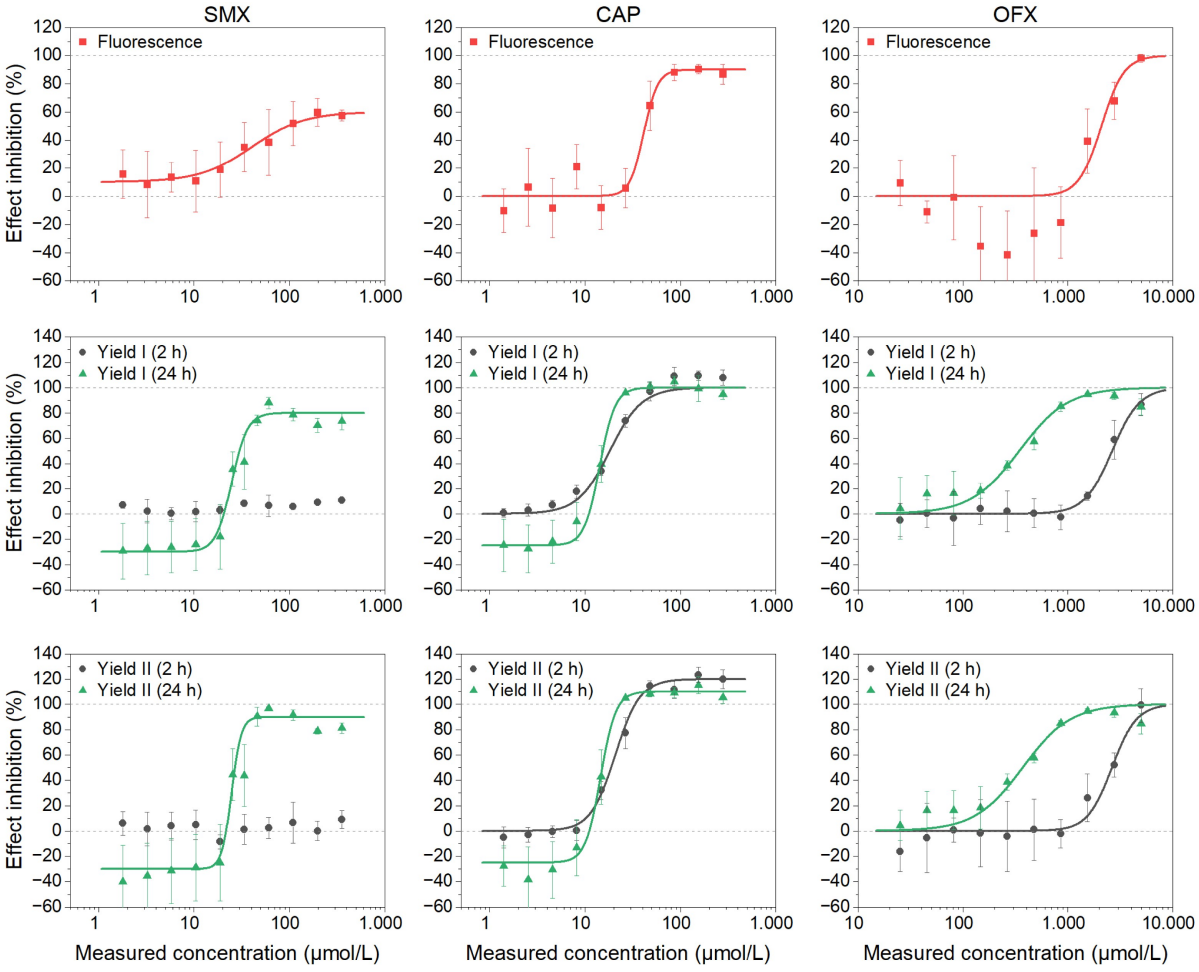


**Fig. 2** Algal toxicity of sulfamethoxazole (SMX, left), chloramphenicol (CAP, center), and ofloxacin (OFX, right) was assessed as the inhibition of algal growth (chlorophyll fluorescence, top), photosynthetic Yield I (center), and photosynthetic Yield II (bottom).

complex effects of OFX on the photosynthesis apparatus, including chloroplast rupture, reduced chlorophyll content, changes in photosynthetic electron transfer and, ultimately, the formation of ROS (Zhang et al., 2023). Deng et al. (2015) reported significant inhibitory effects on the photosynthetic activities of *Microcystis aeruginosa* and weakened protection mechanisms around PSI (cyclic electron flow) at relatively high concentrations of ofloxacin. Thus, effects on the photosystems were observed, supporting the need to use nontarget organisms as a means to evaluate toxin degradation via advanced water treatment techniques.

### 3.2 Removal of antibiotics by a photocatalytic membrane

For photocatalytic membrane treatment of the AB, starting concentrations above the determined $EC_{50}$ or $EC_{80}$ values for at least one of the investigated endpoints were chosen to ensure that the biological test would be able to "follow" the degradation process by the photocatalytic membrane. SMX was used at 10 mg/L (39.5 µmol/L), CAP at 10 mg/L (30.9 µmol/L), and OFX at 1100 mg/L (3044 µmol/L). In addition, OFX was also employed at a relatively low concentration (10 mg/L, 27.7 µmol/L). The data were fitted via the integrated rate law for reactions of $n^{th}$ order (Eq. 3), as shown in Fig 3. The model parameters, characteristic degradation times, and changes in pH (measured before and after 360 min of UV irradiation) are listed in Table 1. The photocatalytic membrane could achieve com-plete parent antibiotic removal. A review by Li et al. (2023b) demonstrated that the photocatalytic membrane removal efficiency for most micropollutants, including antibiotics, falls within the range of 80% to

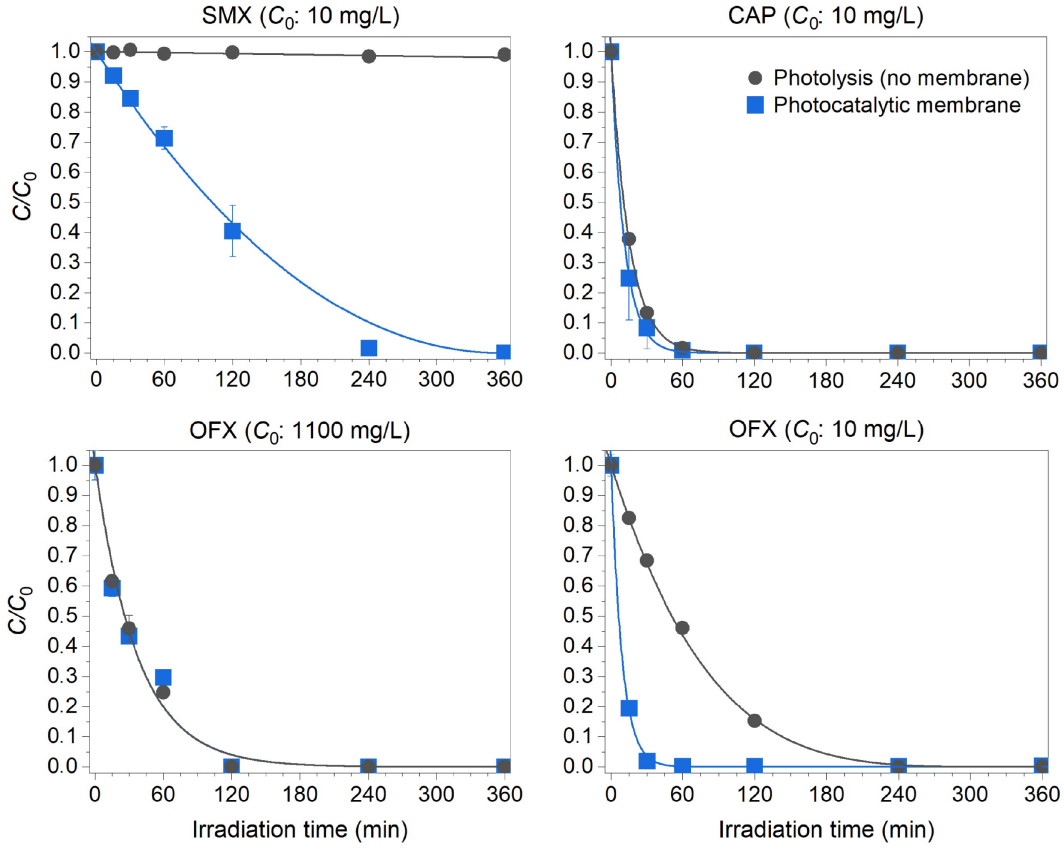


**Fig. 3** Removal of sulfamethoxazole (SMX), chloramphenicol (CAP), and ofloxacin (OFX) via a photocatalytic membrane (■) or photolysis (●) according to HPLC analysis.

100%, whereas CAP could only be removed by about 62%.

Degradation of all AB was supported by a decrease in pH from ~8 to ~3–4, indicating the formation of acidic transformation products as a consequence of oxidative processes. SMX was the only AB that exhibited no significant photolysis within 360 min of irradiation, confirming studies conducted by Kim et al. (2015), *i.e.*, photodegradation is highly dependent on the light source and water chemistry. However, the photocatalytic membrane was capable of degrading 10 mg/L SMX with a half-life of (102.3 ± 5.8) min. A removal of 90% was reached after approximately 241 min. Notably, the total reaction order was found to be $n$ = 0.52, indicating a complex reaction mechanism. However, within the first 60 min, SMX removal followed a pseudo-first-order reaction with an apparent rate constant of $k$ = 0.0056 min$^{-1}$ ($R^2$: 0.999, data not shown). A review by Kutuzova et al. (2021) compiled several studies on the photocatalytic degradation of SMX and reported that pseudo-first-order modeling was most common and that the rate constant decreased in complex water matrices such as wastewater containing large amounts of organic compounds. Hence, in this study, it can be assumed that during UV exposure, photoaging products from the polymer membrane were formed, competing with SMX removal and thus reducing the total apparent reaction order.

TOC analysis supported this hypothesis as the organic carbon content increased during treatment (0 → 360 min): ultrapure water: 1.10 → 58.01 mg/L; SMX: 5.69 → 60.36 mg/L; CAP: 8.61 → 47.11 mg/L; and OFX: 687.35 → 476.73 mg/L. Non-irradiated membranes leached only 5.51 mg/L after 360 min (likely from their hydrophilic coating or the photocatalyst modification layer). Similar self-degradation of PVDF-based photocatalytic membranes has been reported in the literature (Lee et al., 2016; Roubaud et al., 2022; Fischer et al., 2024), explaining the surge in organic carbon. Roubaud et al. (2022) reported that morphological degradation occurs after a few days of irradiation, especially in ultrapure water, since OH radicals are able to attack the membrane instead of solutes. Notably, the increase in the TOC content might be attributable to degradation products of the PVDF polymer or membrane additives. Fischer

**Table 1** Adsorption (Ads), model parameters, and characteristic degradation times for the removal of sulfamethoxazole (SMX), chloramphenicol (CAP), and ofloxacin (OFX) via a photocatalytic membrane or photolysis

| | SMX (10 mg/L) | CAP (10 mg/L) | | OFX (1100 mg/L) | | OFX (10 mg/L) | |
|---|---|---|---|---|---|---|---|
| | Photocat. membrane | Photocat. membrane | Photolysis | Photocat. membrane | Photolysis | Photocat.membrane | Photolysis |
| Ads | 0%±1.2% | 0%±0.3% | 0%±1.7% | 0.1%±4.9% | 4.6%±0.4% | 52.8%±1.7% | 11.8%±2.4% |
| $n$ | 0.52 ±0.10 | 1.0 | 1.0 | 1.0 | 1.0 | 1.0 | 0.78 ±0.04 |
| $k$ | 0.0058±0.0004 | 0.0902±0.0019 | 0.0656±0.0005 | 0.0267±0.0025 | 0.0267±0.0016 | 0.1109±0.0024 | 0.0126±0.0007 |
| $t_{0.5}$ | 102.3±5.8 | 7.7±0.2 | 10.6±0.1 | 26.0±2.5 | 25.9±1.5 | 6.2±0.1 | 51.0±2.3 |
| $t_{0.1}$ | 17.8±1.1 | 1.2±0.0 | 1.6±0.0 | 4.0±0.4 | 3.9±0.2 | 1.0±0.0 | 8.3±0.4 |
| $t_{0.2}$ | 36.8±2.3 | 2.5±0.1 | 3.4±0.0 | 8.4±0.8 | 8.3±0.5 | 2.0±0.0 | 17.3±0.9 |
| $t_{0.8}$ | 194.4±13.2 | 17.9±0.4 | 24.5±0.2 | 60.3±5.7 | 60.1±3.6 | 14.5±0.3 | 107.5±4.0 |
| $t_{0.9}$ | 241.5±20.4 | 25.5±0.5 | 35.1±0.3 | 86.3±8.1 | 86.0±5.1 | 20.7±0.5 | 143.3±5.1 |
| $R^2_{adj.}$ | 1.00 | 1.00 | 1.00 | 0.98 | 0.99 | 1.00 | 0.99 |
| pH | 8.3 → 3.3 | 8.2 → 2.9 | 8.2 → 3.0 | 7.6 → 3.2 | 7.6 → 4.3 | n.d. | n.d. |

Note: No significant photolysis of SMX was observed within 360 min. The change in pH was measured before and after 360 min of UV irradiation. The apparent rate constant of the reaction ($k$) for $n$ = 1 is given in $min^{-1}$, and the characteristic removal times are given in min (*e.g.*, half-life time, $t_{0.5}$, time at 10% removal, $t_{0.1}$, etc.).

et al. (2024) found that the manufacturer's pre-hydrophilization coating is not stable under UV-A irradiation. However, manufacturers often do not disclose the precise hydrophilization agent used. Polyvinylpyrrolidone (PVP), a commonly used membrane additive, is highly sensitive to radical oxidation and may therefore promote the degradation of PVDF (Roubaud et al., 2022). Other studies have confirmed that PVP oxidation occurs first, followed by ROS attacks on the $–CF_2-CH_2–$ segments (Zheng et al., 2023). The main degradation pathway involves dehydrofluorination, whereby PVDF loses hydrogen fluoride (HF) and forms carbon–carbon double bonds (Marshall et al., 2021). CAP was not stable under UV irradiation, yielding an apparent rate constant of 0.0656 $min^{-1}$, whereas the photocatalytic membrane increased the removal rate to 0.0902 $min^{-1}$ (+37%, $t_{0.5}$ = 7.7 min). Similarly, OFX at 1100 mg/L exhibited a strong photolytic reaction, resulting in no difference between photolysis and photocatalysis ($k$ = 0.0267 $min^{-1}$). The literature reports that OFX can act as a photosensitizing agent via the absorption of UV-A radiation, resulting in the formation of singlet and triplet excited states of OFX and, finally, the generation of singlet oxygen (Navaratnam and Claridge, 2007). Most likely, at the employed concentration of 1100 mg/L (which was chosen to monitor the toxicity since OFX was barely toxic toward *S. vacuolatus*), the photosensitizing properties superimposed the photocatalytic degradation, leading to the same apparent rate constant.

Interestingly, at a reduced concentration of 10 mg/L, OFX displayed distinct differences. First, adsorption to the PVDF membrane was much greater at 52.8% (photolysis: 11.8%) than at 1100 mg/L (0.1% ± 4.9% adsorption), indicating that at higher OFX concentrations, adsorption is less relevant (please note that the absolute adsorbed amounts are still comparable). Second, removal by the photocatalytic membrane far exceeded that of photolysis (half-life of 6.2 min *vs* 51.0 min, respectively) and even led to the highest measured rate constant of 0.1109 $min^{-1}$. Finally, the reaction order revealed pseudo-first-order kinetics for the photocatalytic process and fractional-first-order kinetics ($n$ = 0.78) for photolysis. Rytwo and Zelkind (2021) studied the photoconversion of OFX and reported that 20 µmol/L (7.23 mg/L) with no catalyst followed pseudo-order kinetics of ~0.3 with a half-life of about 59 min. However, the sensitivity of the fit was very close within the range of pseudo-orders 0–1. In contrast, Rodríguez et al. (2015) observed only a low conversion after 2 h of UV exposure (370 nm). This finding indicates that photocatalytic polymer membranes can be advantageous for wastewater treatment, exhibiting usually much lower concentrations of micropollutants, as was recently shown for the degradation of steroid hormones (Lotfi et al., 2022; Liu et al., 2023).

### 3.3 Changes in toxicity and identification of transformation products

To evaluate changes in algal toxicity during photocatalytic treatment, samples were collected at various irradiation times to capture the removal profile of the parent compound (Fig. 4), which ideally should be paralleled with a decrease in toxicity. Additionally, ultrapure water was employed as a control to assess any

effects introduced by potential byproducts from the photocatalytic PVDF membrane itself. The data and TOC data indicated that radical-driven photodegradation of the polymer membrane released byproducts was toxic to the algae themselves. All three AB were reduced in concentration (blue lines), and for a more or less short duration, this concentration reduction was followed by a decrease in toxicity (red, green and black lines). However, depending on the AB, after approximately 6–30 min, the toxicity either did not decrease further or even increased again. This would point to the synthesis of transformation products that are more or as toxic as the parent AB or to the additional or rather underlined toxicity produced by photoaging of the pure water used as a technical control. However, OFX toxicity could not be explained by "water toxicity" alone, although the TOC content decreased by ~30%. However, OFX (and potentially its TPs) possessed strong autofluorescence that might have impaired the toxicity assay and thus could explain the observed effect inhibition levels above 100%.

LC-HRMS was employed to identify pre-selected TPs. Figure 5 displays the peak intensities for the parent compounds as well as the observed TPs depending on the irradiation time. The most abundant TPs (according to peak intensity) were highlighted, and their chemical structures were determined: for SMX, the observed TPs peaked at 96–163 min (TP8/9: SMX hydroxylated at either the phenyl or isoxazole group, TP26: 3-amino-5-methylisoxazole); for CAP, the TPs' maximum was between 14-36 min (TP15: 4-nitrobenzoic acid, TP16: 4-nitrophenol); and for OFX, one TP was most abundant, peaking between 6–17 min (TP8: *N*-desmethyl ofloxacin). A detailed overview of the detected TPs is given in the Supporting Information (Tables S7 and S8). This approach is limited by the suspect list, which might miss certain TPs. Assuming that further unidentified TPs follow these trends, the increase in photosynthetic capacity inhibition at the same time points can be supported by the formation of

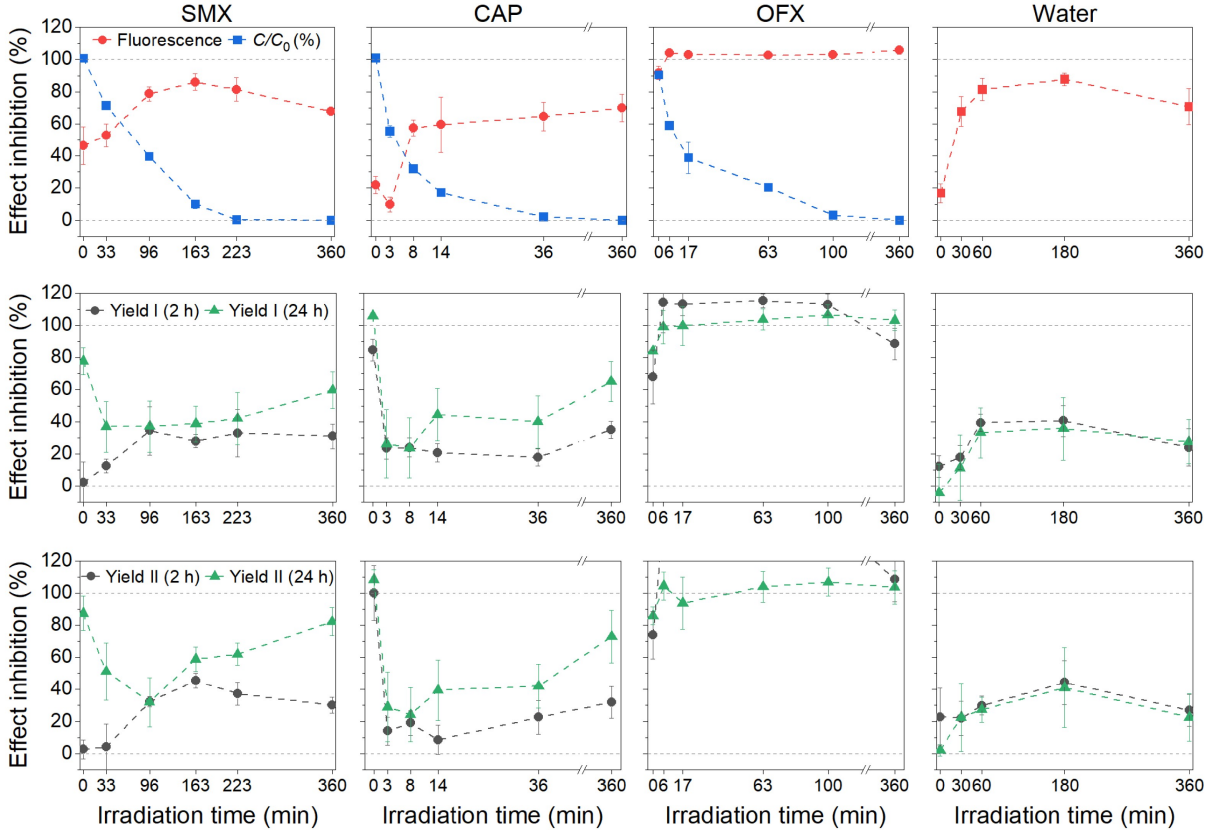


**Fig. 4** Algal toxicity depending on irradiation time for the membrane-based photocatalytic degradation of sulfamethoxazole (SMX, left), chloramphenicol (CAP, center-left), ofloxacin (OFX, center-right), and water (right) at the studied inhibition endpoints, *i.e.*, chlorophyll fluorescence (top), photosynthetic Yield I (center), and photosynthetic Yield II (bottom). The actual concentrations after dilution in the algal toxicity assay ($C/C_0$, in %) are shown on the same axis as fluorescence inhibition (top). Please note the breaks in the x-axis for CAP and OFX.

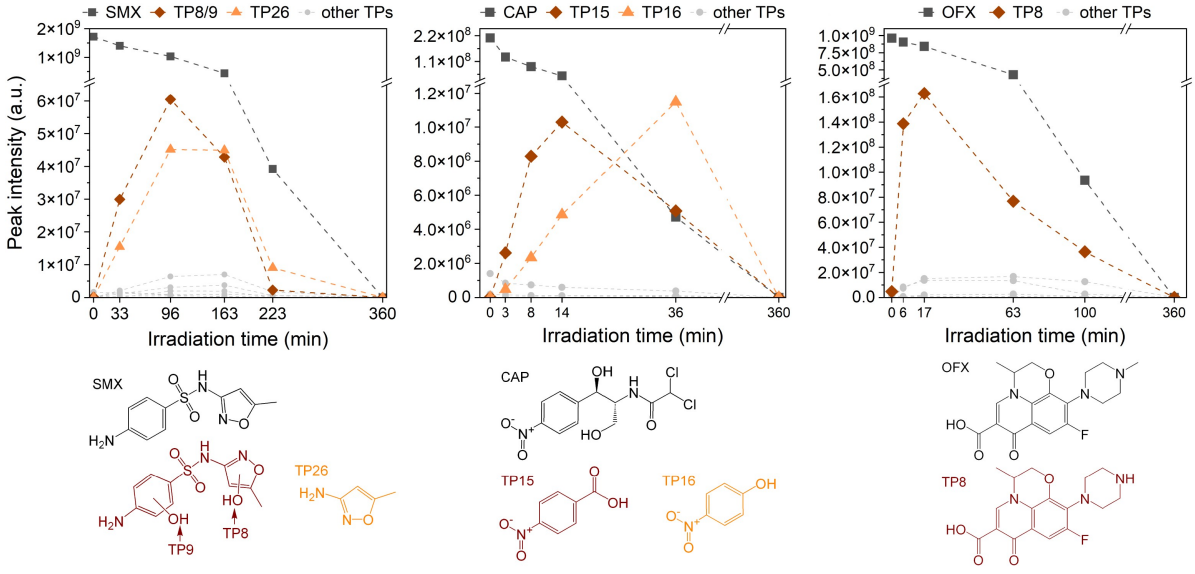


**Fig. 5** Formation of transformation products (TPs) during treatment of sulfamethoxazole (SMX, left), chloramphenicol (CAP, center), and ofloxacin (OFX, right) via the photocatalytic membrane. The chemical structures of the parent compounds and most abundant TPs are displayed below each plot. Please note the breaks in the axes.

toxic degradation products or by the interference of fluorescent but nontoxic degradation products. Owing to the complex mixture containing TPs as well as membrane photoaging products, a correlation between TPs and changes in algal toxicity was not possible. In all the cases, no peak of the parent compound was observed after 360 min of UV exposure.

On the basis of other studies employing pure $TiO_2$ for the photocatalytic degradation of AB, a significant reduction in toxicity is reliable, confirming our results: CAP: residual toxicity of ~10% or lower for the test species *V. fischeri*, *P. subcapitata*, *L. sativum*, and *D. magna* (Lofrano et al., 2016); OFX: reduction in *E. coli* activity by 65%–91% depending on the $TiO_2$ content (Peres et al., 2015). For SMX, studies have reported that both toxification and detoxification depend on the initial concentration, water matrix, and other process factors (Yang et al., 2015; Kutuzova et al., 2021). Ensuring long-term performance and preven-ting secondary ecotoxicity in next-generation photo-catalytic membranes require the development of truly photostable support materials resistant to UV irradiation and attacks by reactive species. Accelerated aging studies have shown that PVDF is one of the more stable support materials for photocatalytic membrane preparation; however, deterioration of hydrophilic additives/coatings is regarded as a significantly more substantial issue (Raota et al., 2023). The majority of studies have focused on changes in material properties, but studies on the toxicological analysis of membrane photoaging products are lacking. Alternative visible-light-active photocatalysts such as $Bi_2WO_6$ have shown exceptional promise, exhibiting few or no photoaging effects on PVDF membranes (Fischer et al., 2024).

## 4 Summary and conclusions

A PVDF polymer membrane coated with $TiO_2$ nanoparticles was used to degrade the antibiotics sulfamethoxazole, chloramphenicol, and ofloxacin under UV irradiation. Toxicity assays with the freshwater alga *Scenedesmus vacuolatus* revealed inhibitory effect concentrations that exceeded typical environmental levels but were in the range of WWTPs. Sulfamethoxazole and chloramphenicol impaired the photosynthetic capacity at 14–25 µmol/L and thus was more sensitive than growth inhibition (~40 µmol/L). Ofloxacin exhibited only low toxicity toward growth inhibition (~2000 µmol/L) but showed a time-dependent increase in photosynthesis inhibition (~2600 µmol/L after 2 h to ~340 µmol/L after 24 h). Photocatalytic membrane treatment of 10–1100 mg/L solutions achieved complete parent-antibiotic removal with half-lives of 6.2–102.3 min, underscoring the effectiveness of the photocatalytic membrane. Thus, the removal efficiency of the used photocatalytic membrane was comparable to or even greater than that of other photocatalytic membranes that have been utilized for the degradation of micropollutants. Monitoring

toxicity at successive irradiation times revealed initial detoxification followed by a resurgence of photosynthetic inhibition due to the formation of toxic transformation products or membrane-derived photoaging products. In general, detoxification is constrained by toxic aging products released from the photocatalytic PVDF membrane. The stability of photocatalytic membranes is presumably limited by the oxidative deterioration of their hydrophilic additives or coating layers under UV irradiation. These findings highlight that, while photocatalytic polymer membranes effectively eliminate antibiotics, their own photostability critically governs secondary ecotoxicity. In contrast to other studies that have focused primarily on changes in material properties, this study emphasizes the need to combine chemical and toxicological methods to reliably validate new methods of wastewater treatment.

**CRediT Authorship Contribution Statement**

Conceptualization, M.S. and E.K.; methodology, M.S., S.A., A.A., M.K. and M.S-J.; formal analysis, M.S., M.K.; investigation, M.S.; resources, A.S. and E.K.; data curation, M.S.; writing–original draft preparation, M.S.; writing–review and editing, M.S., E.K., M.S-J., M.K., and D.B.; visualization, M.S.; supervision, E.K.; project administration, M.S.; funding acquisition, A.S., M.K. and E.K. All authors have read and agreed to the published version of the manuscript.

**Conflict of Interests** The authors declare that they have no known competing financial interests or personal relationships that could have appeared to influence the work reported in this paper.

**Acknowledgements** Dr. Jan Griebel (IOM) is kindly acknowledged for support with the HPLC measurements. The QExactive Plus LC-HRMS used at the UFZ is part of the major infrastructure initiative CITEPro (Chemicals in the Terrestrial Environment Profiler) funded by the Helmholtz Association. Research at the UFZ was also financially supported by the Helmholtz Earth and Environment Program, Topic 9 and Chemicals in The Environment (CITE). This article was prepared as a graduation thesis within the Postgraduate Study Program (PGS) "Toxicology and Environmental Protection" of Leipzig University.

**Electronic Supplementary Material** Supplementary material is available in the online version of this article at https://dx.doi.org/10.1007/s11783-025-2083-7 and is accessible for authorized users.

**Funding Note** Open Access funding enabled and organized by Projekt DEAL.



## References

Abdallah M, Bethäuser J, Tettenborn F, Hein A, Hamann M (2024). Pharmaceutical consumption in human and veterinary medicine in Germany: potential environmental challenges. Frontiers in Environmental Science, 12: 1443935

Ajibola A S, Amoniyan O A, Ekoja F O, Ajibola F O (2021). QuEChERS approach for the analysis of three fluoroquinolone antibiotics in wastewater: concentration profiles and ecological risk in two Nigerian hospital wastewater treatment plants. Archives of Environmental Contamination and Toxicology, 80(2): 389–401

Balbi H J (2004). Chloramphenicol: a review. Pediatrics in Review, 25(8): 284–288

Baran W, Sochacka J, Wardas W (2006). Toxicity and biodegradability of sulfonamides and products of their photocatalytic degradation in aqueous solutions. Chemosphere, 65(8): 1295–1299

Bernhardt A, Lorenz P, Fischer K, Schmidt M, Kühnert M, Lotnyk A, Griebel J, Schönherr N, Zimmer K, Schulze A (2024). Laser-crystallization of $TiO_2$ nanotubes for photocatalysis: influence of laser power and laser scanning speed. Laser & Photonics Reviews, 18(8): 2300778

Chambers M C, Maclean B, Burke R, Amodei D, Ruderman D L, Neumann S, Gatto L, Fischer B, Pratt B, Egertson J, et al. (2012). A cross-platform toolkit for mass spectrometry and proteomics. Nature Biotechnology, 30(10): 918–920

Chen J M, Sun R X, Pan C G, Sun Y, Mai B, Li Q X (2020). Antibiotics and food safety in aquaculture. Journal of Agricultural and Food Chemistry, 68(43): 11908–11919

Chin J Y, Ahmad A L, Low S C (2023). Evolution of photocatalytic membrane for antibiotics degradation: perspectives and insights for sustainable environmental remediation. Journal of Water Process Engineering, 51: 103342

Coulibaly B, Pastor-López E J, Diawara A, Savane F B, Escolà-Casas M, Matamoros V, Ba S (2025). Occurrence of antibiotics in hospital wastewater effluents discharged into the Niger River in Bamako, Mali. Risk assessment and solutions. Environmental Pollution, 371: 125912

Deng C N, Pan X L, Zhang D Y (2015). Influence of ofloxacin on photosystems I and II activities of *Microcystis aeruginosa* and the potential role of cyclic electron flow. Journal of Bioscience and Bioengineering, 119(2): 159–164

Dolar D, Ignjatić Zokić T, Košutić K, Ašperger D, Mutavdžić Pavlović D (2012). RO/NF membrane treatment of veterinary pharmaceutical wastewater: comparison of results obtained on a laboratory and a pilot scale. Environmental Science and Pollution Research, 19(4): 1033–1042

Dührkop K, Fleischauer M, Ludwig M, Aksenov A A, Melnik A V, Meusel M, Dorrestein P C, Rousu J, Böcker S (2019). SIRIUS 4: a rapid tool for turning tandem mass spectra into metabolite structure information. Nature Methods, 16(4): 299–302

Dührkop K, Shen H B, Meusel M, Rousu J, Böcker S (2015). Searching molecular structure databases with tandem mass spectra using CSI:FingerID. Proceedings of the National Academy of Sciences of the United States of America, 112(41): 12580–12585

Felis E, Kalka J, Sochacki A, Kowalska K, Bajkacz S, Harnisz M, Korzeniewska E (2020). Antimicrobial pharmaceuticals in the aquatic environment-occurrence and environmental implications. European Journal of Pharmacology, 866: 172813

Fischer K, Abdul Latif A, Griebel J, Prager A, Shayestehpour O, Zahn S, Schulze A (2024). Immobilization of $Bi_2WO_6$ on polymer membranes for photocatalytic removal of micro-pollutants from water: a stable and visible light active alternative. Global Challenges, 8(3): 2300198

Fischer K, Schulz P, Atanasov I, Abdul Latif A, Thomas I, Kühnert M, Prager A, Griebel J, Schulze A (2018). Synthesis of high crystalline $TiO_2$ nanoparticles on a polymer membrane to degrade pollutants from water. Catalysts, 8(9): 376

Giri A S, Golder A K (2018). Mechanism and identification of reaction byproducts for the degradation of chloramphenicol drug in heterogeneous photocatalytic process. Groundwater for Sustainable Development, 7: 343–347

González-Pleiter M, Gonzalo S, Rodea-Palomares I, Leganés F, Rosal R, Boltes K, Marco E, Fernández-Piñas F (2013). Toxicity of five antibiotics and their mixtures towards photosynthetic aquatic organisms: implications for environmental risk assessment. Water Research, 47(6): 2050–2064

Guo J H, Zhang Y B, Mo J Z, Sun H T, Li Q (2021). Sulfamethoxazole-altered transcriptomein green alga *Raphidocelis subcapitata* suggests inhibition of translation and DNA damage repair. Frontiers in Microbiology, 12: 541451

Gustafson R H, Bowen R E (1997). Antibiotic use in animal agriculture. Journal of Applied Microbiology, 83(5): 531–541

Halling-Sorensen B (2000). Environmental risk assessment of antibiotics: comparison of mecillinam, trimethoprim and ciprofloxacin. Journal of Antimicrobial Chemotherapy, 46(S1): 53–58

Hernández-Tenorio R (2024). Degradation pathways of sulfamethoxazole under phototransformation processes: a data base of the major transformation products for their environmental monitoring. Environmental Research, 262: 119863

Homem V, Santos L (2011). Degradation and removal methods of antibiotics from aqueous matrices: a review. Journal of Environmental Management, 92(10): 2304–2347

Hutchings M I, Truman A W, Wilkinson B (2019). Antibiotics: past, present and future. Current Opinion in Microbiology, 51: 72–80

Kim H Y, Kim T H, Yu S (2015). Photolytic degradation of sulfamethoxazole and trimethoprim using UV-A, UV-C and vacuum-UV (VUV). Journal of Environmental Science and Health, Part A, 50(3): 292–300

Kovalakova P, Cizmas L, McDonald T J, Marsalek B, Feng M B, Sharma V K (2020). Occurrence and toxicity of antibiotics in the aquatic environment: a review. Chemosphere, 251: 126351

Krakowiak R, Musial J, Bakun P, Spychała M, Czarczynska-Goslinska B, Mlynarczyk D T, Koczorowski T, Sobotta L, Stanisz B, Goslinski T (2021). Titanium dioxide-based photocatalysts for degradation of emerging contaminants including pharmaceutical pollutants. Applied Sciences, 11(18): 8674

Kümmerer K (2009). Antibiotics in the aquatic environment: a review. Part I. Chemosphere, 75(4): 417–434

Kusk K O, Christensen A M, Nyholm N (2018). Algal growth inhibition test results of 425 organic chemical substances. Chemosphere, 204: 405–412

Kutuzova A, Dontsova T, Kwapinski W (2021). Application of $TiO_2$-based photocatalysts to antibiotics degradation: cases of sulfamethoxazole, trimethoprim and ciprofloxacin. Catalysts, 11(6): 728

Lee M J, Ong C S, Lau W J, Ng B C, Ismail A F, Lai S O (2016). Degradation of PVDF-based composite membrane and its impacts on membrane intrinsic and separation properties. Journal of Polymer Engineering, 36(3): 261–268

León-Aguirre K, Hernández-Núñez E, González-Sánchez A, Méndez-Novelo R, Ponce-Caballero C, Giácoman-Vallejos G (2019). A rapid and green method for the determination of veterinary pharmaceuticals in swine wastewater by fluorescence spectrophotometry. Bulletin of Environmental Contamination and Toxicology, 103(4): 610–616

Li S, Wu Y N, Zheng H S, Li H B, Zheng Y J, Nan J, Ma J, Nagarajan D, Chang J S (2023a). Antibiotics degradation by advanced oxidation process (AOPs): recent advances in ecotoxicity and antibiotic-resistance genes induction of degradation products. Chemosphere, 311: 136977

Li X H, Liu C, Chen Y X, Huang H K, Ren T Z (2018). Antibiotic residues in liquid manure from swine feedlot and their effects on nearby groundwater in regions of north China. Environmental Science and Pollution Research, 25(12): 11565–11575

Li Y L, Wang X H, Li Z Y, Chen M, Zheng J J, Wang X (2023b). Recent advances in photocatalytic membranes for pharmaceuticals and personal care products removal from water and wastewater. Chemical Engineering Journal, 475: 146036

Liu B Y, Nie X P, Liu W Q, Snoeijs P, Guan C, Tsui M T K (2011). Toxic effects of erythromycin, ciprofloxacin and sulfamethoxazole on photosynthetic apparatus in *Selenastrum capricornutum*. Ecotoxicology and Environmental Safety, 74(4): 1027–1035

Liu S Q, Véron E, Lotfi S, Fischer K, Schulze A, Schäfer A I (2023). Poly(vinylidene fluoride) membrane with immobilized $TiO_2$ for degradation of steroid hormone micropollutants in a photocatalytic membrane reactor. Journal of Hazardous Materials, 447: 130832

Liu Y, Chen S, Zhang J, Li X W, Gao B Y (2017). Stimulation effects of ciprofloxacin and sulphamethoxazole in *Microcystis*

*aeruginosa* and isobaric tag for relative and absolute quantitation - based screening of antibiotic targets. Molecular Ecology, 26(2): 689–701

Lofrano G, Libralato G, Adinolfi R, Siciliano A, Iannece P, Guida M, Giugni M, Volpi Ghirardini A, Carotenuto M (2016). Photocatalytic degradation of the antibiotic chloramphenicol and effluent toxicity effects. Ecotoxicology and Environmental Safety, 123: 65–71

Lotfi S, Fischer K, Schulze A, Schäfer A I (2022). Photocatalytic degradation of steroid hormone micropollutants by $TiO_2$-coated polyethersulfone membranes in a continuous flow-through process. Nature Nanotechnology, 17(4): 417–423

Macdougall J (2006). Analysis of dose–response studies–$E_{max}$ model. In: Ting N, ed. Dose Finding in Drug Development. New York: Springer, 127–145

Maghsodian Z, Sanati A M, Mashifana T, Sillanpää M, Feng S Y, Nhat T, Ramavandi B (2022). Occurrence and distribution of antibiotics in the water, sediment, and biota of freshwater and marine environments: a review. Antibiotics, 11(11): 1461

Marshall J E, Zhenova A, Roberts S, Petchey T, Zhu P C, Dancer C E J, Mcelroy C R, Kendrick E, Goodship V (2021). On the solubility and stability of polyvinylidene fluoride. Polymers, 13(9): 1354

Monk J P, Campoli-Richards D M (1987). Ofloxacin: a review of its antibacterial activity, pharmacokinetic properties and therapeutic use. Drugs, 33(4): 346–391

Murray C J L, Ikuta K S, Sharara F, Swetschinski L, Robles Aguilar G, Gray A, Han C, Bisignano C, Rao P, Wool E, et al. (2022). Global burden of bacterial antimicrobial resistance in 2019: a systematic analysis. The Lancet, 399(10325): 629–655

Nasrollahi N, Vatanpour V, Khataee A (2022). Removal of antibiotics from wastewaters by membrane technology: limitations, successes, and future improvements. Science of the Total Environment, 838: 156010

Navaratnam S, Claridge J (2007). Primary photophysical properties of ofloxacin. Photochemistry and Photobiology, 72(3): 283–290

OECD (2006). Test No. 201: Freshwater Alga and Cyanobacteria, Growth Inhibition Test. Paris: Organization for Economic Co-operation and Development

Pauletto M, De Liguoro M (2024). A review on fluoroquinolones' toxicity to freshwater organisms and a risk assessment. Journal of Xenobiotics, 14(2): 717–752

Peres M S, Maniero M G, Guimarães J R (2015). Photocatalytic degradation of ofloxacin and evaluation of the residual antimicrobial activity. Photochemical & Photobiological Sciences, 14(3): 556–562

Raota C S, Lotfi S, Lyubimenko R, Richards B S, Schäfer A I (2023). Accelerated ageing method for the determination of photostability of polymer-based photocatalytic membranes. Journal of Membrane Science, 686: 121944

Rigano L, Schmitz M, Linnemann V, Krauss M, Hollert H, Pfenninger M (2025). Exposure to complex mixtures of urban sediments containing tyre and road wear particles (TRWPs) increases the germ-line mutation rate in *Chironomus riparius*. Aquatic Toxicology, 281: 107292

Rodil R, Moeder M, Altenburger R, Schmitt-Jansen M (2009). Photostability and phytotoxicity of selected sunscreen agents and their degradation mixtures in water. Analytical and Bioanalytical Chemistry, 395(5): 1513–1524

Rodríguez E M, Márquez G, Tena M, Álvarez P M, Beltrán F J (2015). Determination of main species involved in the first steps of $TiO_2$ photocatalytic degradation of organics with the use of scavengers: the case of ofloxacin. Applied Catalysis B: Environmental, 178: 44–53

Rodriguez-Mozaz S, Chamorro S, Marti E, Huerta B, Gros M, Sànchez-Melsió A, Borrego C M, Barceló D, Balcázar J L (2015). Occurrence of antibiotics and antibiotic resistance genes in hospital and urban wastewaters and their impact on the receiving river. Water Research, 69: 234–242

Roubaud E, Maréchal W, Lorain O, Lamaa L, Peruchon L, Brochier C, Mendret J, Mericq J P, Brosillon S, Faur C, et al. (2022). Understanding aging mechanisms in the context of UV irradiation of a low fouling and self-cleaning PVDF-PVP-$TiO_2$ hollow-fiber membrane. Membranes, 12(5): 538

Rummel C D, Schäfer H, Jahnke A, Arp H P H, Schmitt-Jansen M (2022). Effects of leachates from UV-weathered microplastic on the microalgae *Scenedesmus vacuolatus*. Analytical and Bioanalytical Chemistry, 414(4): 1469–1479

Rytwo G, Zelkind A L (2021). Evaluation of kinetic pseudo-order in the photocatalytic degradation of ofloxacin. Catalysts, 12(1): 24

Schmid R, Heuckeroth S, Korf A, Smirnov A, Myers O, Dyrlund T S, Bushuiev R, Murray K J, Hoffmann N, Lu M S, et al. (2023). Integrative analysis of multimodal mass spectrometry data in MZmine 3. Nature Biotechnology, 41(4): 447–449

Schmitt-Jansen M, Bartels P, Adler N, Altenburger R (2007). Phytotoxicity assessment of diclofenac and its phototransformation products. Analytical and Bioanalytical Chemistry, 387(4): 1389–1396

Smilack J D (1999). Trimethoprim-sulfamethoxazole. Mayo Clinic Proceedings, 74(7): 730–734

UBA (2021). Database-Pharmaceuticals in the Environment [Online]. Dessau-Roßlau: The Umweltbundesamt Office

Wang C L (2018). Fractional kinetics of photocatalytic degradation. Journal of Advanced Dielectrics, 8(5): 1850034

WHO Scientific Working Group (1983). Antimicrobial resistance. Bulletin of the World Health Organization, 61(3): 383–394

Xiong Q, Hu L X, Liu Y S, Wang T T, Ying G G (2019). New insight into the toxic effects of chloramphenicol and roxithromycin to algae using FTIR spectroscopy. Aquatic Toxicology, 207: 197–207

Xu Q, Song Z J, Ji S T, Xu G, Shi W Y, Shen L X (2019). The photocatalytic degradation of chloramphenicol with electrospun $Bi_2O_2CO_3$-poly(ethylene oxide) nanofibers: the synthesis of crosslinked polymer, degradation kinetics, mechanism and cytotoxicity. RSC Advances, 9(51): 29917–29926

Yang C C, Huang C L, Cheng T C, Lai H T (2015). Inhibitory effect

of salinity on the photocatalytic degradation of three sulfonamide antibiotics. International Biodeterioration & Biodegradation, 102: 116–125

Zhang Z H, Liu X N, Li N, Cao B L, Huang T T, Li P, Liu S Q, Zhang Y Z, Xu K (2023). Effect of ofloxacin levels on growth, photosynthesis and chlorophyll fluorescence kinetics in tomato. Plant Physiology and Biochemistry, 194: 374–382

Zheng X, Dai D Y, Hua H L, Yu D W, Cheng R, Zheng L B (2023). Aging behavior and mechanism of polyvinylidene fluoride membrane by intensified UV irradiation and NaOCl: a comparative study. Process Safety and Environmental Protection, 180: 923–934